J Physiol 587.7 (2009) pp 1593–1605

The Journal of Physiology

Examination of 'lipotoxicity' in skeletal muscle of high-fat fed and *ob*/*ob* mice

S. M. Turpin[1], J. G. Ryall[3], R. Southgate[4], I. Darby[5], A. L. Hevener[6], M. A. Febbraio[7], B. E. Kemp[1], G. S. Lynch[3] and M. J. Watt[1,2]

[1] *St Vincent's Institute of Medical Research and the Department of Medicine, University of Melbourne, Fitzroy, Australia, 3065*
[2] *Biology of Lipid Metabolism Laboratory, Department of Physiology, Monash University, Clayton, Victoria, Australia, 3800*
[3] *Basic and Clinical Myology Laboratory, Department of Physiology, University of Melbourne, Australia, 3010*
[4] *The Peter MacCallum Cancer Institute, East Melbourne, Australia, 3002*
[5] *School of Medical Sciences, RMIT University, Bundoora, Australia, 3083*
[6] *David Geffen School of Medicine, Division of Endocrinology, Diabetes and Hypertension University of California, Los Angeles, CA 90095, USA*
[7] *Cellular and Molecular Metabolism Laboratory, Baker IDI Heart and Diabetes Institute, 75 Commercial Rd, Melbourne, Victoria, Australia, 3004*

Excess lipid accumulation resulting from an elevated supply of plasma fatty acids is linked to the pathogenesis of the metabolic syndrome and heart disease. The term 'lipotoxicity' was coined to describe how lipid accumulation leads to cellular dysfunction and death in non-adipose tissues including the heart, pancreas and liver. While lipotoxicity has been shown in cultured skeletal muscle cells, the degree of lipotoxicity *in vivo* and the functional consequences are unresolved. We studied three models of fatty acid overload in male mice: 5 h Intralipid® and heparin infusion, prolonged high fat feeding (HFF) and genetic obesity induced by leptin deficiency (*ob*/*ob* mice). Markers of apoptosis, proteolysis and autophagy were assessed as readouts of lipotoxicity. The Intralipid® infusion increased caspase 3 activity in skeletal muscle, demonstrating that enhancing fatty acid flux activates pro-apoptotic pathways. HFF and genetic obesity increased tissue lipid content but did not influence apoptosis. Gene array analysis revealed that HFF reduced the expression of 31 pro-apoptotic genes. Markers of autophagy (LC3β and beclin-1 expression) were unaffected by HFF and were associated with enhanced Bcl_2 protein expression. Proteolytic activity was similarly unaffected by HFF or in *ob*/*ob* mice. Thus, contrary to our previous findings in muscle culture *in vitro* and in other non-adipose tissues *in vivo*, lipid overload did not induce apoptosis, autophagy or proteolysis in skeletal muscle. A broad transcriptional suppression of pro-apoptotic proteins may explain this resistance to lipid-induced cell death in skeletal muscle.

(Received 25 November 2008; accepted after revision 2 February 2009; first published online 9 February 2009)
Corresponding author M. J. Watt: Department of Physiology, Monash University, Clayton, Victoria, Australia, 3800. Email: matthew.watt@med.monash.edu.au

Obesity is defined by increased lipid storage in visceral and subcutaneous adipose tissue, but a secondary complication is ectopic lipid deposition in non-adipose tissues. This occurs as a consequence of increased adipose tissue lipolysis (Horowitz *et al.* 1999), delivery of free fatty acids (FFAs) and triglycerides (Bickerton *et al.* 2008) to peripheral tissues and an increased sarcolemmal fatty acid transport (Bonen *et al.* 2004). Lipid accumulation in non-adipose cells can cause cell dysfunction or cell death via apoptosis, and these processes have been broadly defined as 'lipotoxic' (Unger, 2003). While the pathogenic consequences of excessive lipid deposition are well described for the pancreas, heart and liver (Shimabukuro *et al.* 1998; Sparangna & Hickson-bick, 2000; Garris, 2005; Summers, 2006; Wei *et al.* 2006), they remain poorly described in skeletal muscle.

Skeletal muscle represents the largest metabolically active tissue in the body and accounts for approximately 40% of body mass. Skeletal muscle contributes a large proportion of whole-body fatty acid uptake and oxidation (van der Vusse & Reneman, 1996) as well as 75–90% of insulin-stimulated glucose disposal (Baron *et al.* 1988). Analogous to the lipotoxicity reported in the pancreas and liver, the surplus fatty acid delivery to and storage in skeletal muscle may also initiate intracellular signalling events to alter muscle function, size and morphology. Obesity is characterised by increases in circulating lipids (FFAs, triglycerides) that accumulate

DOI: 10.1113/jphysiol.2008.166033

in muscle as triacylglycerol and fatty acid metabolites such as ceramide, diacylglycerol and long chain acyl CoA (Adams *et al.* 2004; Watt *et al.* 2006*a*). We have previously shown that saturated fatty acids induce *de novo* ceramide accumulation and apoptosis in cultured myotubes (Turpin *et al.* 2006) while others reported the induction of apoptotic signalling after 16 weeks of high fat, high-sucrose feeding in rodents (Bonnard *et al.* 2008). Aside from this report, the importance of fatty acid overload in mediating lipotoxicity *in vivo* is not described.

Skeletal muscle is a remarkably adaptive tissue that is composed of heterogeneous muscle fibres that differ in their contractile and metabolic profile. Type I fibres contain slow isoforms of contractile proteins and have an enhanced capacity for mitochondrial respiration and fatty acid oxidation, whereas type II fibres exhibit fast twitch contractile properties and preferentially oxidise glucose (Fluck & Hoppeler, 2003). A striking feature of the myofibre is the ability to transform and remodel in response to changing environmental demands. A classic example of skeletal muscle remodelling is endurance exercise training, which invokes intracellular signalling pathways (Bassel-Duby & Olson, 2006) and consequent genetic reprogramming that leads to pronounced changes in biochemical, morphological and physiological characteristics of individual myofibres (Holloszy, 1967). Obese humans possess fewer type I muscle fibres and more type IIb muscle fibres compared with lean humans (Lillioja *et al.* 1987; Houmard *et al.* 2002) and genetically obese *ob*/*ob* mice have a striking reduction in muscle mass and a reduced ability to undergo hypertrophy (Almond & Enser, 1984; Warmington *et al.* 2000). It is not known whether these differences in muscle morphology are determined genetically or result from changes in cellular processes and remodelling associated with 'obesogenic' environmental influences, such as fatty acid overload. Understanding the mechanisms involved in myofibre remodelling is particularly relevant to several metabolic disorders (e.g. obesity, type 2 diabetes) because increasing the abundance of type I fibres is associated with enhanced fatty acid metabolism, protection against glucose intolerance (Lin *et al.* 2002; Ryder *et al.* 2003) and resistance to muscle wasting (Minnaard *et al.* 2005).

The first aim of the present study was to define whether fatty acid overload in skeletal muscle influences lipotoxic cellular pathways involved in cell death and protein degradation. Specifically, we evaluated apoptosis, proteasome activity and markers of autophagy in several models of chronic fatty acid overload. The second aim was to carefully assess muscle mass and fibre type composition with high fat feeding. We hypothesized that fatty acid overload would induce apoptosis and proteolysis and promote skeletal muscle remodelling towards a glycolytic phenotype.

Methods

Animal experimental procedures

All experimental protocols were approved by St Vincent's Hospital Melbourne (SVHM) Animal Ethics Committee. Male C57Bl6/J mice at 8 weeks of age (Monash Animal Services, Clayton, Australia) were fed a high fat diet (HFD, 45% calories from fat, Specialty Feeds, Glen Forrest, Australia) or standard rodent chow (Chow, 9% fat) for either 1 day, or 1, 4 and/or 12 weeks (total mice used = 90). This design allowed us to investigate signalling during the progression of obesity, which we have defined as an increase in fat pad mass. *ob*/*ob* mice and littermate controls were obtained from Monash Animal Services (Clayton, Australia) at 10 weeks of age and maintained on standard rodent chow (total *ob*/*ob* mice used was 16). ATGL null mice were generated as described (Haemmerle *et al.* 2006) and studied at 10 weeks of age (total ATGL mice used was 8). All mice were anesthetized with an intraperitoneal injection of pentobarbital sodium (60 mg kg^{-1} Nembutal; Boehringer Inglheim Pty Ltd, Aratanonon, Australia) at 11.00 h after fasting for 1–3 h. Blood was obtained via cardiac puncture, centrifuged at 8000 *g* for 5 min and the plasma snap frozen. The extensor digitorum longus (EDL) and soleus (SOL) muscles were carefully dissected, placed onto a mould and covered in optimal cutting temperature gel. Muscles were then placed in liquid nitrogen cooled isopentane for 5–10 s then snap frozen for later analysis. Mixed gastrocnemius (GAST) and vastus (VAST) muscles, and epididymal (EPI), retro-peritoneal (RET) and subcutaneous (SC) adipose tissues were dissected, weighed and snap frozen in liquid nitrogen. Tibialis anterior (TA) muscles were fixed in 4% paraformaldehyde for 16–24 h and stored at 4°C in 70% ethanol before being embedded in paraffin. All mice were killed by cervical dislocation at the end of experiments.

In other experiments, C57Bl/6 mice were anesthetized as described and the jugular vein was catheterized with micro-renthane (MRE 0.025; Braintree Scientific, Braintree, MA, USA). The indwelling catheter was tunnelled subcutaneously, exteriorized at the back of the neck and encased in Silastic tubing. Four days after surgery, mice underwent a 5 h saline (Saline) or triacylglycerol (TG) emulsion and heparin infusion (Lipid, 20% Intralipid®, heparin 20 U ml^{-1}, 0.1 ml h^{-1}). At the conclusion of the infusion, mice were anesthetized and blood was drawn via cardiac puncture. Tissues were dissected and snap frozen as described.

Plasma metabolites and hormones

Whole blood was centrifuged for 5 min at 8000 *g* and the plasma removed. Free fatty acids were determined by enzymatic colorimetric assay (Wako NEFA C test kit, Wako

Chemicals, VA, USA) and glucose by the glucose oxidase method (Sigma-Aldrich, St Louis, MO, USA).

Muscle lipid analysis

Triacylglycerols were extracted from freeze dried GAST as previously described (Watt *et al.* 2006b) and saponified, and glycerol was assessed (Free Glycerol Reagent, Sigma-Aldrich). Diacylglycerol and ceramide were extracted and quantified by a diacylglycerol kinase linked radiometric assay (Preiss *et al.* 1986).

Histology and immunohistochemistry

Cross-sections of SOL and EDL muscles were cut on a Shandon SME cryostat (6 μm), adhered to silane-coated microscopic slides and stained to determine fibre morphology, fibre type distribution and DNA fragmentation (described later). Images of sections were produced by an Axio Ziess Imager D1 Microscope and analysed by the same operator in single blinded manner using AxioVision 4.6 software.

Hematoxylin and eosin staining

Muscle sections were stained with hematoxylin and eosin to determine general muscle architecture, the percentage of fibres with centrally located nuclei, and the cross-sectional area (CSA) of individual myofibres.

Myosin ATPase staining

Myosin ATPase reactivity was determined as described (Ryall *et al.* 2002). Serial sections were pre-incubated at pH 4.33 and 4.54 to identify type I, IIa and IIb muscle fibre types. After the procedure, sections were dehydrated in xylene and coverslips applied. Muscle fibres were classified according to their mATPase activity by interactive determination of fibre histochemical reaction intensity (Hamalainen & Pette, 1993).

Terminal deoxynucleotidyl transferase dUTP nick end labelling (TUNEL)

TUNEL was used to determine fragmented DNA in paraffin-embedded TA muscle sections according to the manufacturer's guidelines (DeadEnd TUNEL kit, Promega, Madison, WI, USA). For quantification, five random images were obtained at $\times$20 magnification and the TUNEL index (TUNEL positive nuclei/Total nuclei) was calculated for each field in a set area in a double-blinded manner.

Fluorometric caspase 3 activity assay

GAST muscle lysates were prepared and DEVD-caspase was assayed by cleavage of Ac-DEVD-AFC (Ac-asp-glu-val-asp-7-amino-4-trifluoromethylcoumarin), a fluorogenic substrate based on the peptide sequence at the caspase-3 cleavage site of poly(adenosine diphosphate-ribose) polymerase (Findlay *et al.* 2002). Lysate from staurosporine treated C2C12 myotubes was used as a positive control.

Proteasome activity

To determine ubiquitin-proteasome-dependent protein breakdown of contractile proteins, proteasomes were extracted and activity of chymotrypsin-like, trypsin-like and caspase-like activity measured as described (Minnaard *et al.* 2005). Proteasomes were extracted from VAST muscle and activity of the proteasome was assessed using chymotrypsin-like and trypsin-like specific substrates (Suc-LLVY-AMC no. 6510, Boc-LRR-AMC no. B4643, Z-LLE-AMC no. C0483) with and without an inhibitor (MG132 no. C2211) to assess the proteasome-dependant activity. The substrates and inhibitor were purchased from Sigma-Aldrich. The fluorescence of samples and a positive control (20S Proteasome from rabbit, no. P3988, Sigma-Aldrich) were continuously monitored (λ excitation 380 nm and λ emission 440 nm; POLARstar, BMG Labtech, Mornington, Victoria, Australia). Results were corrected for MG132 sensitivity [RFU ($-$MG132) $-$ RFU ($+$MG132) $=$ MG132 sensitive RFU] before determining the rate of reaction. The slope of the linear distribution equals the rate of hydrolysis of the substrate expressed in RFU (μg protein)$^{-1}$ min^{-1}.

Western blotting

Freeze dried GAST muscle was lysed and protein concentration determined (bicinchoninic acid method; Pierce Kit no. 23225, Quantum Scientific, QLD, Australia). Lysates were solubilized, resolved by SDS PAGE on 10–16% polyacrylamide gels, transferred to nitrocellulose membranes and blocked with 5% milk. Immunoblotting was performed using the following primary antibodies: anti-caspase 3 from BioVision (Mountain View, CA, USA), anti-phospho-Ser^{9} and total GSK3β and anti-actin from Sigma-Aldrich (St Louis, MO, USA), total mTOR from Cell Signalling Technology (Beverly, MA, USA), ubiquitin (P4D1) from Santa Cruz Biotechnology (Santa Cruz, CA, USA) anti-bax (Ab-5) and anti Bcl-$_2$ (Ab-4) from Oncogene (San Diego, CA, USA). After incubation with protein G-HRP secondary antibody (Bio-Rad, Hercules, CA, USA), the immunoreactive proteins were detected with enhanced chemiluminescence and quantified by densitometry (Image J, NIH).

RNA extraction and real-time quantitative PCR

Total RNA was extracted from mixed vastus muscle in Qiazol extraction reagent followed by isolation using an RNeasy kit (Qiagen, Doncaster, Victoria, Australia). RNA quantity was determined (NanoDrop p2000 Spectrometer, Biolab, Australia). Reverse transcription of mRNA was performed using the thermoscript RT-PCR system (Invitrogen, Mount Waverly, Australia) with random hexamer priming. Gene products were determined by real-time quantitative RT-PCR (Stratagene Mx3000P, La Jolla, CA, USA) using a Super Array RT^2 Profiler PCR Array system (Bioscience Corp., Frederick, MD, USA, no. 1022B), which contains 84 apoptosis focused primer sets with five housekeeping and three RNA and PCR quality control genes. PCR conditions were 10 min at 95°C followed by 40 cycles of PCR reaction at 95°C for 15 s and 60°C for 60 s. Actb was used as a reference gene and did not vary between groups. The mRNA levels were determined by a comparative C_T method. For each sample, a ΔC_T value was obtained by subtracting Actb C_T values from those of the apoptotic gene of interest. The average ΔC_T value of the lean group was then subtracted from the sample to derive a $\Delta - \Delta C_T$ value. The expression of each gene was then evaluated by $2-(\Delta - \Delta C_T)$. For all other mRNA analysis the primer sets were purchased from Applied Biosystems (Foster City, CA, USA).

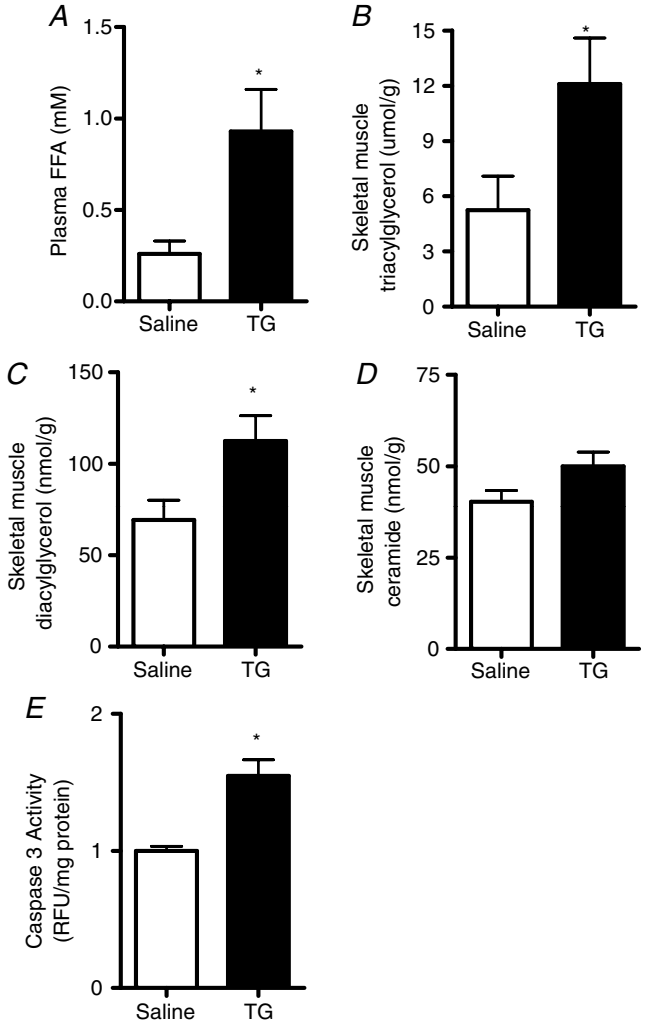

Figure 1. Acute elevation of plasma free fatty acids causes muscle lipid accumulation and activates pro-apoptotic signalling
Catheterized mice were infused with saline (Saline) or a triacylglycerol and heparin solution (TG) for 5 h. *A*, plasma FFA was determined after 5 h. *B–D*, triacylglycerol (*B*), diacylglycerol (*C*) and ceramide (*D*) were determined in mixed gastrocnemius muscles. *E*, caspase 3 activity was determined in muscle lysates prepared from the same tissue. $^*P < 0.05$, $n = 5$ for each group.

Statistical analysis

Data are presented as means ± standard error of the mean (S.E.M.). Differences between groups were determined by two-way ANOVA with repeated measures or Student's unpaired *t*-test. $P \leq 0.05$ was considered statistically significant.

Results

Evidence that acute fatty acid oversupply can induce pro-apoptotic signalling

Fatty acids induce apoptosis in culture skeletal muscle myotubes (Turpin *et al.* 2006). The purpose of the initial experiments was to determine whether acute increases in FA can induce skeletal muscle apoptosis *in vivo*. Plasma FFAs were artificially elevated by acute triglyceride and heparin infusion into lean mice. As expected, plasma FFAs were increased (Fig. 1*A*) after 5 h Intralipid® and heparin infusion while myocellular triacylglycerol (Fig. 1*B*) and diacylglycerol were also increased (Fig. 1*C*). Skeletal muscle ceramides tended to increase ($P = 0.10$, Fig. 1*D*). Caspase 3 activity was increased by 55% with lipid infusion (Fig. 1*E*), demonstrating that acute fatty acid oversupply can induce pro-apoptotic signalling similar to that shown in myotubes *in vitro* (Turpin *et al.* 2006).

Chronic lipid overload does not increase apoptosis in skeletal muscle

Having established that fatty acids can induce apoptotic signalling in cultured skeletal muscle myotubes (Turpin *et al.* 2006) and in mice acutely (Fig. 1), we then assessed apoptosis in several models of chronic fatty acid overload. Body mass, adipose tissue mass (Table 1), and intramyocellular and liver triacylglycerol content (Table 1) were elevated after 12 weeks' HFD. Muscle diacylglycerol was increased with HFD and there was no change in muscle ceramide (Table 1). Plasma FFAs

Table 1. Fat mass, tissue lipid content and blood metabolites in murine models of obesity

	Chow	HFD	Lean	*ob*/*ob*
Body mass (g)	30.5 ± 0.8	34.1 ± 0.9*	27.0 ± 0.4	47.2 ± 5.2*
Epididymal fat (g)	0.87 ± 0.15	1.68 ± 0.27*	0.66 ± 0.07	1.92 ± 0.40*
Subcutaneous fat (g)	0.45 ± 0.09	1.10 ± 0.17*	0.14 ± 0.04	1.01 ± 0.08*
Retroperitoneal fat (g)	0.26 ± 0.06	0.61 ± 0.12*	0.41 ± 0.07	3.64 ± 0.25*
Liver TAG (μmol g^{-1})	11.9 ± 1.9	36.1 ± 8.4*	2.9 ± 0.9	10.7 ± 4.3
Muscle TAG (μmol g^{-1})	6.5 ± 1.1	13.1 ± 2.2*	4.7 ± 1.8	51.7 ± 6.9*
Muscle DAG (nmol g^{-1})	328 ± 31	453 ± 47*	68 ± 12	179 ± 45*
Muscle ceramide (nmol g^{-1})	191 ± 21	184 ± 20	40 ± 6	95 ± 18*
Plasma FFA (μM)	223 ± 71	289 ± 45	148 ± 21	375 ± 160
Plasma glucose (mM)	13.0 ± 1.5	11.9 ± 1.2	15.4 ± 1.6	17.3 ± 0.9
Plasma insulin (pM)	302 ± 77	816 ± 197*	448 ± 146	2822 ± 47*

Data are presented as mean ± S.E.M. $n = 8$ for Chow and HFD, $n = 8$ for Lean and *ob*/*ob*. *$P < 0.05$. DAG, diacylglycerol; TAG, triacylglycerol.

and glucose were not different between Chow and HFD, which reflected the post-prandial state of the mice. The *ob*/*ob* mice had elevated plasma FFAs, extreme adipose tissue deposition and increased intramyocellular and liver triacylglycerol levels compared with littermates controls (Table 1). Collectively, these results indicate that lipid overload is a characteristic of the HFD and *ob*/*ob* mice.

We used several approaches to assess apoptosis in skeletal muscle. Caspase 3 activity (Fig. 2*A* and *B*) and DNA fragmentation were not affected by HFD at any

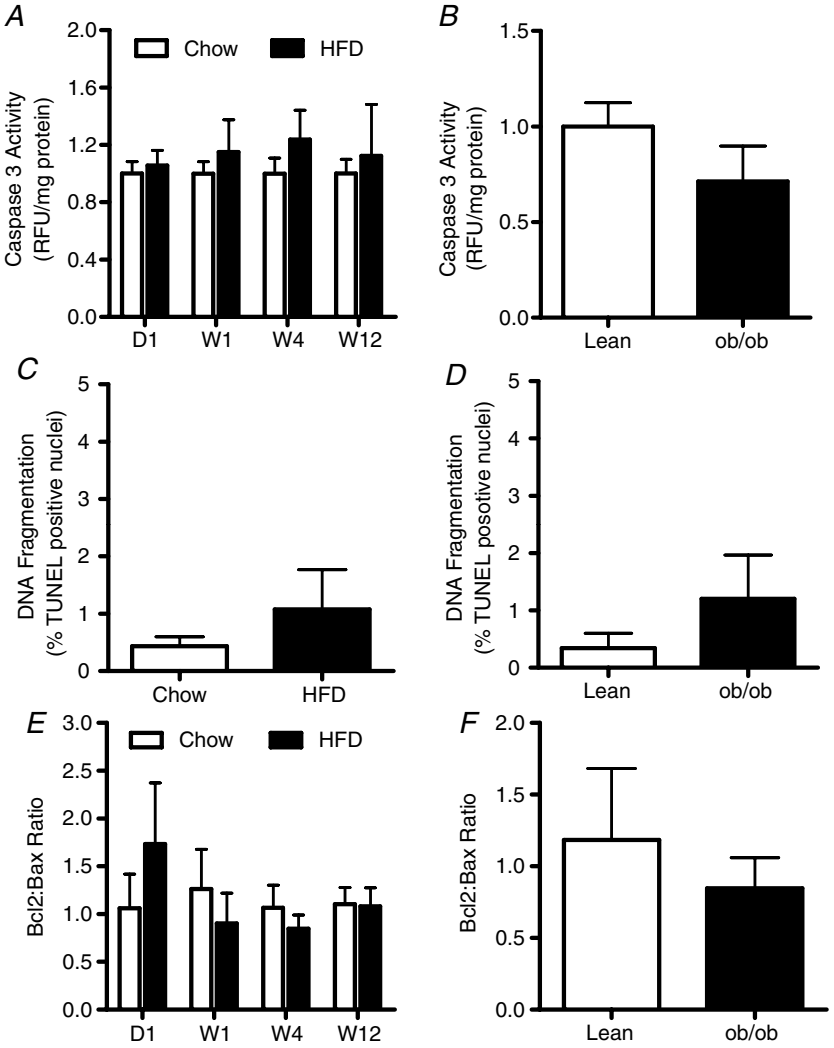

Figure 2. Apoptosis in skeletal muscle is not elevated in dietary or genetic obesity
Mixed gastrocnemius and tibialis anterior muscles were excised from mice fed a low-fat (Chow) or high-fat diet (HFD) for 1 day (D1), 1 week (W1), 4 weeks (W4) or 12 weeks (W12). Tissue lysates or sections were assessed for caspase 3 activity (*A*), DNA fragmentation as assessed by the percentage of TUNEL positive nuclei from embedded tibialis anterior muscle (*C*) and the Bcl_2: Bax ratio by Western blot (*E*). $n = 8$ for both groups. Similar analysis were performed in muscles of *ob*/*ob* mice and lean littermate controls (*B*, *D* and *F*). $n = 8$ for both groups.

time point examined in HFD mice (Fig. 2*C*) or in *ob*/*ob* mice (Fig. 2*D*). The Bcl_2: Bax ratio represents the propensity for cellular apoptosis and was not different with HFD (Fig. 2*E*) or in *ob*/*ob* mice (Fig. 2*F*). We also investigated apoptosis in ATGL null mice, which is a good model to assess lipotoxicity because skeletal muscle lipid content is elevated by ∼450% (muscle triglyceride, wild-type (WT): 3.8 ± 0.8 *vs.* ATGL null: 17.8 ± 3.8 umol g^{-1}, $P = 0.004$, muscle ceramide, WT: 72 ± 10 *vs.* ATGL null: 95 ± 22 pmol mg^{-1}, $P = 0.43$, $n = 6$). Caspase 3 activity was not different between ATGL null mice and wild-type littermates (WT: 6.5 ± 0.8 *vs.* ATGL null: 5.1 ± 0.6 RFU (mg protein)$^{-1}$, $P = 0.24$, $n = 6$ for each group).

Although chronic fat oversupply did not appear to induce apoptosis in skeletal muscle, it was possible that we mistimed our measurements. Accordingly, we assessed muscle fibre regeneration by analysing random muscle cross-sections for centrally located nuclei. Muscle fibre regeneration was not increased by HFD (central nuclei: Chow 2.8 ± 1.9 *vs.* HFD 6.0 ± 2.4, $P = 0.32$, $n = 7$). Together, these findings demonstrate that apoptosis is not increased with chronic lipid overload in skeletal muscle *in vivo*.

High fat feeding suppresses transcription of pro-apoptotic proteins

Increased fatty acid deposition in non-adipose tissues such as the liver and pancreas increase the expression and activity of key pro-apoptotic signalling proteins (Unger *et al.* 1999; Garris, 2005). Having previously demonstrated lipoapoptosis in skeletal muscle cells *in vitro* (Turpin *et al.* 2006), we were surprised with the absence of apoptosis *in vivo*. Since the acute fatty acid-infusion model induced pro-apoptotic signalling *in vivo* (Fig. 1), we hypothesized that the resistance to apoptosis with HFD was related to transcriptional adaptations that may have diminished pro-apoptotic outcomes. We profiled 84 apoptosis-related genes in the skeletal muscle of Chow and HFD mice (Table 2). One-third of the pro-apoptotic genes were down-regulated ($P < 0.05$) in response to a HFD. The most noteworthy of these were mitochondrial proteins Bcl_{10}, Bok and Bad, and stimulators of chromatin condensation, Dffb and caspase 6. Caspase 3 was the only pro-apoptotic gene up-regulated by HFD; however, the transcriptional increase did not translate into greater protein content (data not shown) or activity (Fig. 2*A*). Several pro-apoptotic genes were unchanged including the death domain genes Fadd, Fas, Fasl and caspases 1, 2, 4, 7, 8, 12 and 14. Interestingly, the pro-apoptotic genes which were down-regulated in response to HFD are predominately associated with the mitochondria and the nucleus. These organelles are well known to induce apoptotic signalling via several pathways responsible for the commitment of a cell to death.

Chronic lipid overload does not affect skeletal muscle proteolysis *in vivo*

Proteolysis is the directed degradation of proteins by cellular proteases after ubiquitin is tagged to proteins marked for degradation. The proteasome is a multicatalytic complex that degrades substrates into small peptides via different peptidase activities (i.e. chymotrypsin-like, trypsin-like and caspase-like). FOXO1 activation has been suggested to increase the transcription of MAFbx and MuRF-1, and thereby the activation of ubiquitin-proteasome mediated muscle proteolysis (Stitt *et al.* 2004). Since FOXO1 is elevated under conditions where fatty acid availability is increased (i.e. starvation; Furuyama *et al.* 2003), we investigated the effects of HFD on FOXO1, muscle-specific ubiquitin ligase expression and proteolytic activity. Expression of MAFbx, MuRF-1 and FOXO1 were not increased with HFD (Table 3) and the HFD did not affect the ubiquitination of proteins (Fig. 3*A*). Chymotrypsin-like activity was decreased (Fig. 3*B*) but trypsin-like (Fig. 3*C*) and caspase-like (Fig. 3*D*) proteolytic activity were not affected with HFD. In *ob*/*ob* mice, FOXO1 mRNA was upregulated but was not associated with changes in MAFbx or MuRF-1 (Table 3). There was no evidence of accelerated proteolysis in skeletal muscle of *ob*/*ob* mice (Fig. 3*E*–*H*).

Chronic lipid overload does not affect skeletal muscle autophagy *in vivo*

Autophagy is a recently identified process that describes the degradation of cellular proteins via the lysosomal degradation pathway. Autophagy regulates cell growth, development and overall homeostasis by balancing the synthesis, degradation and recycling of cellular products. To our knowledge this is the first study to assess autophagy in skeletal muscle of obese mice. Beclin-1 initiates the development of the vesicle membrane around the autophagasome and regulates the union of LC-3α and β to the autophagasome membrane (Pattingre *et al.* 2008). Beclin-1 mRNA was not affected by HFD (Fig. 4*A*) but was increased 2-fold in the *ob*/*ob* mouse (Fig. 4*B*). Bcl_2 prevents beclin-1 regulation of autophagasome formation by directly binding and preventing vesicle nucleation and was elevated by HFD (Chow 1.00 ± 0.11 *vs.* HFD 2.16 ± 0.53, $P < 0.05$), perhaps explaining the absence of beclin-1 induction with HFD and not in *ob*/*ob* mice (Bcl_2: Lean, 1.00 ± 0.49 *vs.* ob/ob 1.25 ± 0.23, $P = 0.64$). LC-3α and -β are markers of isolation membrane formation, LC-3β is formed upon the union of LC-3α to phosphatidylethanolamine on the inside of the

Table 2. Differential expression of apoptotic genes in mice fed a high-fat diet

Gene function	Gene name	Pro/anti apoptotic	Fold change	*P* value
Death domain				
Casp8	Caspase 8	Pro	−2.22	0.08
Casp14	Caspase 14	Pro	−1.11	0.21
Cflar	Caspase 8 and FADD-like apoptosis regulator	Pro	−1.49	0.17
Fadd	Fas (TNFRSF6) – associated via death domain	Pro	−1.32	0.08
Tnf	Tumour necrosis factor	Pro	−4.76	0.01*
Tnfsf10	Tumour necrosis factor (ligand) superfamily member 10	Pro	−3.03	0.03*
Tnfrsf10b	Tumour necrosis factor superfamily member 10b	Pro	−2.00	0.11
Tnfrsf11b	Tumour necrosis factor superfamily member 10b	Anti	−9.09	0.11
Traf1	Tnf receptor-associated factor 1	Pro	−5.88	0.01*
Traf2	Tnf receptor-associated factor 2	Pro	−1.72	0.11
Traf3	Tnf receptor-associated factor 3	Pro	−1.67	0.10
Mitochondrial				
Bad	Bcl-associated death promoter	Pro	−2.38	0.05*
Bak1	Bcl2-antagonist/killer 1	Pro	−4.00	0.15
Bcl2	B-cell leukemia/lymphoma 2	Anti	−3.13	0.01*
Bcl10	B-cell leukemia/lymphoma 10	Pro	−1.79	0.02*
Bcl_2l10	Bcl2-like 10	Pro	−3.33	0.02*
Bid	BH3 interacting domain death agonist	Pro	−2.38	0.05*
Bok	Bcl-2-related ovarian killer protein	Pro	−3.03	0.02*
Pim2	Proviral integration site 2	Anti	−7.69	0.04*
Nucleic				
Casp 6	Caspase 6	Pro	−2.56	0.04*
Dffa	DNA fragmentation factor, alpha subunit	Anti	1.71	0.13
Dffb	DNA fragmentation factor, beta subunit	Pro	−3.33	0.03*
Hells	Helicase, lymphoid specific	Anti	−2.56	0.08
NfkB1	Nuclear factor of kappa light chain gene enhancer of B-cells 1, p105	Anti/Pro	−1.47	0.13
Pycard	PYD & CARD domain containing	Pro	−4.35	0.02*
Trp53bp2	Transformation related protein 53 binding protein 2	Anti	−1.12	0.33
Trp73	Transformation related protein 73	Pro	−3.57	0.03*
Cytosolic				
Apaf1	Apoptotic peptidase activating factor 1	Pro	−3.03	0.08
Birc1a	Baculoviral IAP repeat-containing 1a	Anti	−2.70	0.07
Birc3	Baculoviral IAP repeat-containing 3	Anti	−1.69	0.04*
Birc5	Survivin	Anti	−6.67	0.21
Casp1	Caspase 1	Pro	−2.50	0.08
Casp2	Caspase 2	Pro	−2.08	0.13
Casp3	Caspase 3	Pro	7.49	0.04*
Casp4	Caspase 4	Pro	−3.23	0.11
Casp7	Caspase 7	Pro	−2.33	0.09
Casp12	Caspase 12	Pro	−1.43	0.19
Gusb	Glucuronidase, beta	Pro	−1.85	0.14
Hsp90ab1	Heat shock protein 90 kDa α (cytosolic), class B member1	Anti	−1.49	0.14
Other				
Cd40lg	CD40 ligand	Anti/Pro	−5.88	0.11
Cd70	CD70 antigen	Pro	−2.78	0.12
Cidea	Cell death-inducing DNA fragmentation factor, alpha subunit-like effector A	Pro	−0.29	0.80
Cideb	Cell death-inducing DNA fragmentation factor, alpha subunit-like effector B	Pro	−2.86	0.12
Dapk1	Death associated protein kinase 1	Anti	2.22	0.33
Il10	Interleukin 10	Anti	−7.14	0.11
Lhx4	LIM homeobox protein 4	Anti	−2.70	0.10
Nme5	Expressed in non-metastatic cells 5	Anti	−4.35	0.02*
Zc3hc1	Zinc finger, C3HC type 1	Anti	−2.56	0.09

mRNA quality was assessed by measuring the 260/280 ratio: Chow 1.88 ± 0.05 *vs.* HFD 1.89 ± 0.05, $P = 0.93$, $n = 6$. $^*P < 0.05$ HFD *vs.* Chow.

Table 3. Gene expression in HFD and *ob*/*ob* mice compared with lean controls

Gene	Chow	HFD	Lean	*ob*/*ob*
MAFbx	1.03 ± 0.10	1.30 ± 0.26	1.06 ± 0.28	1.25 ± 0.35
MuRF1	1.08 ± 0.18	1.13 ± 0.21	1.00 ± 0.36	1.34 ± 0.28
FOXO1	1.08 ± 0.16	1.61 ± 0.35	1.04 ± 0.36	3.81 ± 1.29*
mTOR	1.02 ± 0.07	1.53 ± 0.21	1.01 ± 0.24	1.85 ± 0.56

Values are expressed as mean ± S.E.M., $n = 8$ for each group. *$P < 0.05$ *vs.* Lean.

autophagosomal membrane. Once the membrane is formed, all autophagy proteins are recycled into the cytosol except for LC-3β. Accordingly, lipidated LC-3β (i.e. the activated/processed form) is a key marker of autophagy. We found no increase in LC-3β mRNA content with HFD (Fig. 4*C*), but detected a 2-fold increase in the *ob*/*ob* mouse (Fig. 4*D*). FOXO proteins have been reported to drive the expression of LC-3α and β in muscle (Mammucari *et al.* 2007; Zhao *et al.* 2007). Consistent with this notion, FOXO1 mRNA was elevated in *ob*/*ob* mice but not by HFD (Table 3). Further analysis revealed that LC-3βI and LC-3βII (activated form) protein was not different between Chow and HFD (Fig. 4*C*) or lean and *ob*/*ob* mice (Fig. 4*D*). The conserved nutrient-responsive TOR signalling pathway is also a critical regulator of autophagy. mTOR gene expression was not increased with lipid oversupply (Table 3) and mTOR activity was not different between groups as assessed by phosphorylation of its substrate p70 S6K1 at Thr^{389} (Fig. 4*E* and *F*). It is important to note that S6 kinase does not mediate TOR's effects on autophagy, but is a marker of TOR activity. Collectively, these data indicate an upregulation of the necessary components to drive the autophagic process in *ob*/*ob* mice but not with high fat feeding.

Muscle fibre determination and analysis of atrophy and hypertrophy genes

Although controversial, some studies have reported that human and rodent obesity is characterized by a decrease in overall muscle mass and greater proportion of glycolytic type IIb muscle fibres (Almond & Enser, 1984; Lillioja *et al.* 1987; Houmard *et al.* 2002). To investigate this further, we assessed whether prolonged lipid overload was associated with a shift towards a glycolytic phenotype and a smaller muscle mass. There was no diet-induced change in the fibre type distribution (Fig. 5*A*); however, an increase in the mean area for type I, IIa and IIb fibres was observed in soleus muscle with HFD (Fig. 5*B*). There was no difference in fibre type distribution or fibre size in the EDL muscles (data not shown).

Discussion

'Lipotoxicity' is a commonly used term that broadly describes detrimental changes to cell morphology and function induced by an excess of fatty acids and/or intracellular accumulation of lipids that may cause cell death. There is no doubt that lipotoxicity, as originally defined, is evident in the pancreas, liver and possibly the heart (Shimabukuro *et al.* 1998; Sparangna & Hickson-bick, 2000; Garris, 2005; Summers, 2006; Wei *et al.* 2006). Likewise, lipid overload undoubtedly disrupts some aspects of skeletal muscle function, such as insulin signal transduction. This study was undertaken to specifically determine whether an excess of lipids causes apoptosis, autophagy or proteolysis in skeletal muscle, and whether these events are related to changes in muscle morphology. Our studies indicate that acute fatty acid overload can promote pro-apoptotic signalling; however, apoptosis, autophagy and proteolysis are not elevated in chronic models of 'lipotoxicity'.

Extensive evidence shows that saturated fatty acids can induce apoptosis in several cell types including pancreatic β-cells, hepatocytes, cardiomyocytes and skeletal muscle myotubes *in vitro* (Shimabukuro *et al.* 1998; Sparangna & Hickson-bick, 2000; Turpin *et al.* 2006; Wei *et al.* 2006). Fatty acid-induced apoptosis, or 'lipoapoptosis', causes changes in tissue function. For example, insulin secretion from β-cells is impaired following apoptosis in the pancreas (Shimabukuro *et al.* 1998). The primary aim of the present study was to extend on our previous work in cultured muscle cells (Turpin *et al.* 2006) and examine apoptosis in skeletal muscle *in vivo*. Our results indicate that an acute elevation of fatty acids increases lipid deposition in skeletal muscle and activates caspase 3, a key pro-apoptotic initiator. The cause of the acute caspase 3 activation is unknown but could involve several factors known to be elevated with lipid oversupply including TNFR activation (Uysal *et al.* 1997), NFκB activation (Sinha *et al.* 2004) and Fas ligand activation (Lee *et al.* 2007). In response to chronic HFD or in *ob*/*ob* mice there was no evidence of accelerated apoptosis or increased muscle regeneration/degeneration. The absence of apoptosis was surprising in light of our previous studies in cultured myotubes (Turpin *et al.* 2006) and the current studies with acute Intralipid® infusion in mice showing pro-apoptotic effects of fatty acids. The absence of apoptosis with 12 weeks' high fat feeding contrasted with an earlier study by Bonnard *et al.* (2008), which demonstrated pro-apoptotic signalling after 16 weeks of high-fat, high-sucrose feeding that induced marked oxidative stress and apoptosis. Thus, it is possible that a longer dietary regime or a combination of lipo- and glucotoxicity is required to induce apoptosis *in vivo*, although this would seem unlikely given that the severely hyerlipidaemic/hyperglycaemic *ob*/*ob* mouse

does not exhibit pronounced apoptosis. These studies also reveal a disconnect between ceramide accumulation and apoptosis in *ob*/*ob* mice, suggesting that, unlike cultured muscle cells where ceramide accumulation was essential for fat-induced apoptosis (Turpin *et al.* 2006), ceramide accumulation is not mandatory for apoptosis *in vivo*.

The absence of lipoapoptosis in intact skeletal muscle may result from a rapid down-regulation of pro-apoptotic

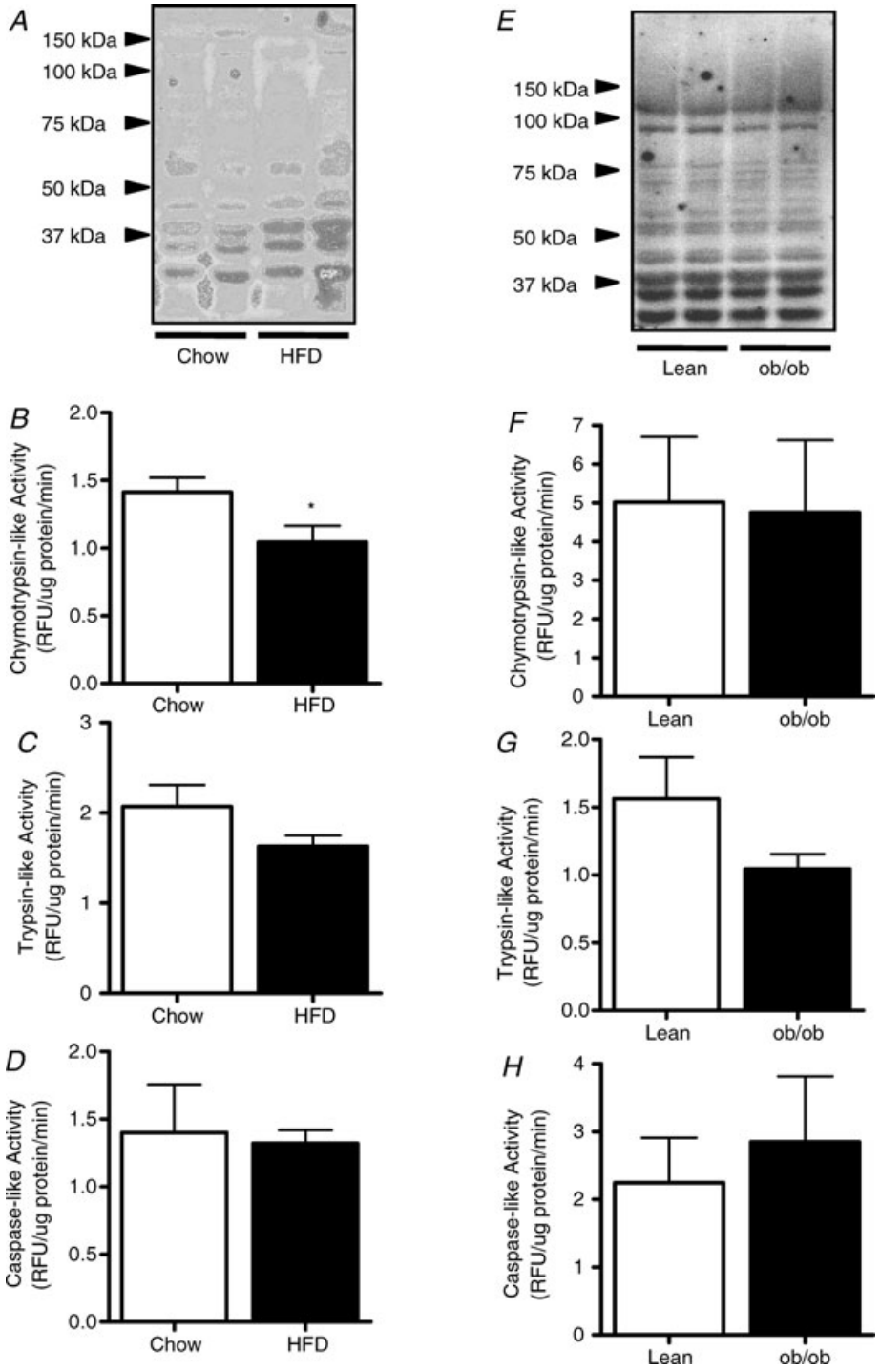

Figure 3. Skeletal muscle proteolysis in obese mice
Muscle ubiquitination (*A*), chymotrypsin-like activity (*B*), trypsin-like activity (*C*) and caspase-like activity (*D*) were determined in skeletal muscle lysates of mice fed a low-fat (Chow) or high-fat diet (HFD) for 12 weeks. Analysis of muscle ubiquitination (*E*), chymotrypsin-like activity (*F*), trypsin-like activity (*G*) and caspase-like activity (*H*) were performed in muscles of *ob*/*ob* mice and lean littermate controls. $^*P < 0.05$ Chow *vs*. HFD, $n = 8$ for both groups.

proteins. A large proportion of pro-apoptotic genes were down-regulated in high-fat fed obese mice compared with lean mice, indicating that a molecular adaptation to lipid oversupply is the generalized suppression of pro-apoptotic genes, which prevents lipoapoptosis in skeletal muscle. It should be noted that several anti-apoptotic genes were also downregulated, although the biological significance of this response remains unclear. Overall, these conclusions parallel those of Ghosh *et al.* (2004), which showed marked pro-apoptotic actions of fatty acids resulting in cardiotoxicity *in vitro*, but negligible cardiomyocyte apoptosis *in vivo*. Thus, this and previous studies Shimabukuro *et al.* 1998; Sparangna & Hickson-bick, 2000; Garris, 2005; Summers, 2006; Wei *et al.* 2006) suggest that there is a hierarchy of susceptibility to lipoapoptosis *in vivo*, with pancreas and liver being highly susceptible and heart and skeletal muscle being largely refractory to lipoapoptosis. Interesting, this hierarchy is also reflective of the oxidative capacity of these tissues indicating that oxidative disposal of fatty acids may be important in affording protection against lipoapoptosis.

Eukaryotes have evolved to use autophagy to control events such as cellular remodelling during development, programmed cell death, and the turnover of damaged organelles to provide metabolic substrates during starvation (Maiuri *et al.* 2007). One function of autophagy is to alleviate endoplasmic reticulum (ER) stress and thereby diminish apoptotic cell death (Ding *et al.* 2007). Since high-fat feeding is associated with inflammation (Wellen & Hotamisligil, 2005) and ER stress (Ozcan *et al.* 2004), we hypothesized that autophagy would be up-regulated to prevent ER stress, and inflammatory and pro-apoptotic signalling that is associated with fatty acid oversupply (Boya *et al.* 2005; Degenhardt *et al.* 2006; Ding *et al.* 2007). While autophagy was detected in skeletal muscles of mice, this was not exacerbated with the HFD. This response could be explained by an increase in Bcl_2 protein expression, which is known to suppress beclin-1

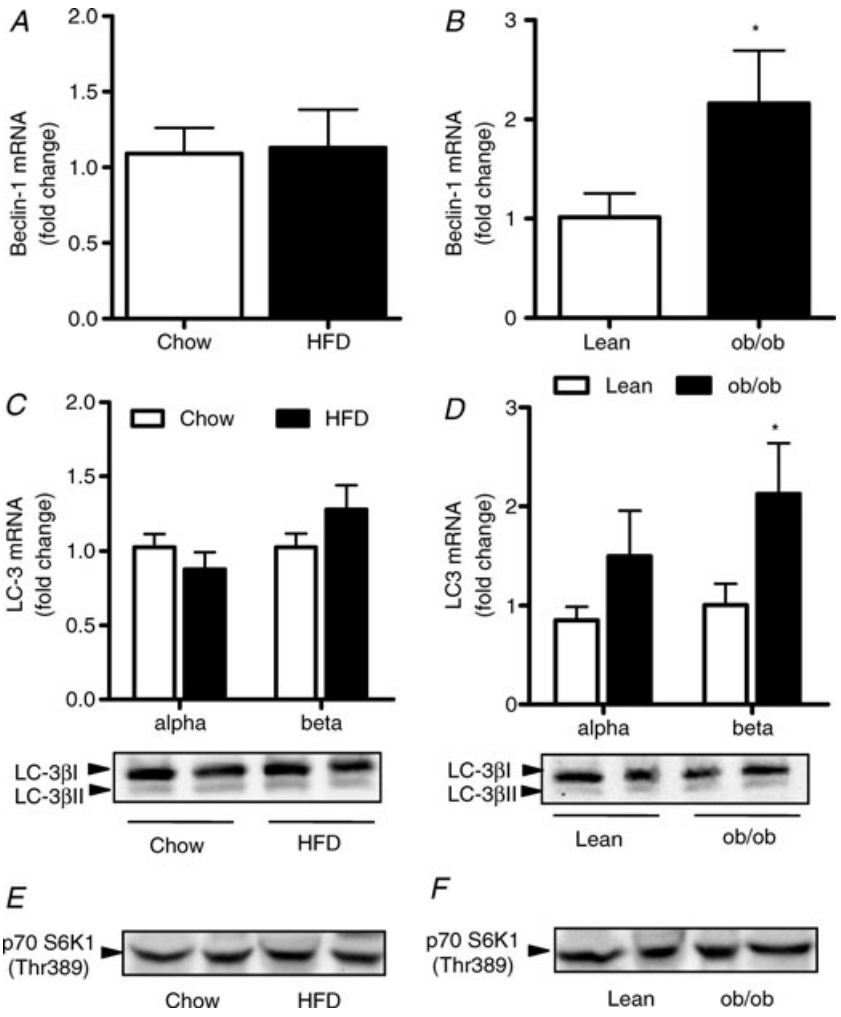

Figure 4. Skeletal muscle autophagy in obese mice
Mixed gastrocnemius muscle was excised from mice fed a low-fat (Chow) or high-fat diet (HFD) for 12 weeks. RNA was extracted, reverse transcribed and quantitative RT-PCR was performed to assess mRNA expression for beclin-1 (*A*) and LC-3α and LC-3β (*C*). A second aliquot of muscle was homogenized and protein expression of LC-3βI and LC-3βII (*C*) and p70 S6K1 Thr^{389} (*E*). $^*P < 0.05$, $n = 8$ for both groups. Similar analysis were performed in muscles of *ob/ob* mice and lean littermate controls (*B*, *D* and *H*). $n = 8$ for all groups.

and autophagy initiation (Pattingre *et al.* 2005). Inhibition of this process prevents phagosome membrane formation and LC-3α and -β expression. This interpretation is supported by our findings in *ob*/*ob* mice of increased beclin-1 and LC-3β mRNA expression in the absence of Bcl_2 induction. In contrast to the HFD model, *ob*/*ob* mice exhibited an upregulation of the necessary components to drive the autophagic process. To our knowledge this is the first study to show FOXO1 and LC-3β upregulation in skeletal muscle of obese mice, which is consistent with a stimulatory role of FOXO proteins in driving the expression of LC-3β in muscle (Mammucari *et al.* 2007; Zhao *et al.* 2007). Together, these results provide novel evidence that autophagic pathways can be activated in some models of obesity; however, enhancing Bcl_2 expression may prevent these events in skeletal muscle *in vivo*.

Mass and fibre size in adult skeletal muscle is regulated by responses to workload, activity and/or pathological conditions (Stitt *et al.* 2004). Increased muscle loading enhances protein synthesis and results in muscle hypertrophy (Goldspink *et al.* 1983) while ubiquitination of proteins by the muscle-specific ubiquitin ligases, MAF_{bx} and MuRF1, results in eventual protein degradation via the 26S proteasome complex (Jagoe & Goldberg, 2001). Previous studies have shown reduced muscle mass and impaired hypertrophy in genetically obese mice (Almond & Enser, 1984) while the term 'sarcopenic obesity' describes a combination of excess weight and reduced muscle mass in humans (Dominguez & Summer 2007). A better understanding of the mechanisms which lead from loss of muscle mass to obesity or from obesity to muscle loss is important from a public health perspective. To investigate this relationship, we examined skeletal muscle fibre area, proteolysis and hypertrophy/atrophy signalling. We observed a small but significant increase in type I, IIa and IIb muscle fibre areas in response to the HFD, with no change in the proportion of fibre types within the soleus muscle. No such changes were observed in the EDL muscle. These differences are likely to be explained by the function of these muscles; the soleus is a postural muscle and is therefore subject to the increased load associated with an increased body mass with HFD. The unexpected increase in soleus muscle fibre area with HFD was associated with decreased chymotrypsin and trypsin-like activities of the 26S proteasome. The biochemical/molecular adaptations mediating this response are presently unclear. MAF_{bx} and MuRF1, which are specific constituents of muscle and play a critical role in protein loss, were not down-regulated with lipid overload. Similarly, FOXO1 is a transcription factors for key atrophy-related genes (Lee *et al.* 2004) and was unchanged. Finally, there was no increase in the conjugation of ubiquitin to muscle proteins while caspase 3, which provides substrates for the ubiquitin-proteasome pathway, was not activated. Thus, the series of events typically associated with atrophy were not down-regulated in obesity. Also, hypertrophic signalling via mTOR, S6K and GSK3β was not activated (data not shown).

In conclusion, these observations suggest that unlike isolated cultured systems and other non-adipose tissues, lipid oversupply is not a major factor determining skeletal muscle apoptosis, autophagy and proteolysis, discrete events that control cellular death and remodelling, respectively. The protection against the pro-apoptotic effects of fatty acids is associated with a generalized down-regulation of pro-apoptotic genes, while an increase in Bcl_2 may be important in preventing autophagy. The present study also highlights the importance of performing *in vivo* studies to validate the applicability/physiological relevance of signalling pathways and cellular events identified *in vitro*.

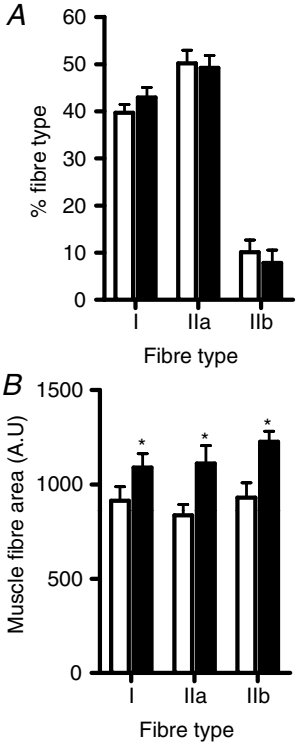

Figure 5. High-fat feeding is associated with increased muscle mass
Soleus muscle was excised from mice fed a low-fat (Chow) or high-fat diet (HFD) for 12 weeks. Muscles were fixed and 6 μm sections were reacted for mATPase for muscle fibre type determination (*A*). The area of individual fibres was determined (*B*). $^*P < 0.05$, $n = 8$ for both groups.

References

Adams JM, Pratipanawatr T, Berria R, Wang E, DeFronzo RA, Sullards MC & Mandarino LJ (2004). Ceramide content is increased in skeletal muscle from obese insulin-resistant humans. *Diabetes* **53**, 25–31.

Almond RE & Enser M (1984). A histochemical and morphological study of skeletal muscle from obese hyperglycaemic ob/ob mice. *Diabetologia* **27**, 407–413.

Baron AD, Brechtel G, Wallace P & Edelman SV (1988). Rates and tissue sites of non-insulin- and insulin-mediated glucose uptake in humans. *Am J Physiol Endocrinol Metab* **255**, E769–774.

Bassel-Duby R & Olson EN (2006). Signaling pathways in skeletal muscle remodeling. *Annu Rev Biochem* **75**, 19–37.

Bickerton AS, Roberts R, Fielding BA, Tornqvist H, Blaak EE, Wagenmakers AJ, Gilbert M, Humphreys SM, Karpe F & Frayn KN (2008). Adipose tissue fatty acid metabolism in insulin-resistant men. *Diabetologia* **51**, 1466–1474.

Bonen A, Parolin ML, Steinberg GR, Calles-Escandon J, Tandon NN, Glatz JF, Luiken JJ, Heigenhauser GJ & Dyck DJ (2004). Triacylglycerol accumulation in human obesity and type 2 diabetes is associated with increased rates of skeletal muscle fatty acid transport and increased sarcolemmal FAT/CD36. *FASEB J* **18**, 1144–1146.

Bonnard C, Durand A, Peyrol S, Chanseaume E, Chauvin MA, Morio B, Vidal H & Rieusset J (2008). Mitochondrial dysfunction results from oxidative stress in the skeletal muscle of diet-induced insulin-resistant mice. *J Clin Invest* **118**, 789–800.

Boya P, Gonzalez-Polo R-A, Casares N, Perfettini J-L, Dessen P, Larochette N, Metivier D, Meley D, Souquere S, Yoshimori T, Pierron G, Codogno P & Kroemer G (2005). Inhibition of macroautophagy triggers apoptosis. *Mol Cell Biol* **25**, 1025–1040.

Degenhardt K, Mathew R, Beaudoin B, Bray K, Anderson D, Chen G, Mukherjee C, Shi Y, Gélinas C, Fan Y, Nelson DA, Jin S & White E (2006). Autophagy promotes tumor cell survival and restricts necrosis, inflammation, and tumorigenesis. *Cancer Cell* **10**, 51–64.

Ding W-X, Ni H-M, Gao W, Yoshimori T, Stolz DB, Ron D & Yin X-M (2007). Linking of autophagy to ubiquitin-proteasome system is important for the regulation of endoplasmic reticulum stress and cell viability. *Am J Pathol* **171**, 513–524.

Dominguez LJ & Barbagallo M (2007). The cardiometabolic syndrome and sarcopenic obesity in older persons. *J Cardiometab Syndr* **2**, 183–189.

Findlay D, Raggatt L, Bouralexis S, Hay S, Atkins G & Evdokiou A (2002). Calcitonin decreases the adherence and survival of HEK-293 cells by a caspase-independent mechanism. *J Endocrinol* **175**, 715–725.

Fluck M & Hoppeler H (2003). Molecular basis of skeletal muscle plasticity: from gene to form and function. *Rev Physiol Biochem Pharmacol* **146**, 159–216.

Furuyama T, Kitayama K, Yamashita H & Mori N (2003). Forkhead transcription factor FOXO1 (FKHR)-dependent induction of PDK4 gene expression in skeletal muscle during energy deprivation. *Biochem J* **375**, 365–371.

Garris D (2005). Cytochemical analysis of pancreatic islet lipoapoptosis: hyperlipidemia-induced cytoinvolution following expression of the diabetes (db/db) mutation. *Pathobiology* **72**, 124–123.

Ghosh S, An D, Pulinilkunnil T, Qi D, Lau HC, Abrahani A, Innis SM & Rodrigues B (2004). Role of dietary fatty acids and acute hyperglycemia in modulating cardiac cell death. *Nutrition* **20**, 916–923.

Goldspink D, Garlick P & McNurlan MA (1983). Protein turnover measured in vivo and in vitro in muscles undergoing compensatory growth and subsequent denervation atrophy. *Biochem J* **210**, 89–98.

Haemmerle G, Lass A, Zimmermann R, Gorkiewicz G, Meyer C, Rozman J, Heldmaier G, Maier R, Theussl C, Eder S, Kratky D, Wagner EF, Klingenspor M, Hoefler G & Zechner R (2006). Defective lipolysis and altered energy metabolism in mice lacking adipose triglyceride lipase. *Science* **312**, 734–737.

Hamalainen N & Pette D (1993). The histochemical profiles of fast fiber types IIB, IID, and IIA in skeletal muscles of mouse, rat, and rabbit. *J Histochem Cytochem* **41**, 733–743.

Holloszy JO (1967). Biochemical adaptations in muscle. Effects of exercise on mitochondrial oxygen uptake and respiratory enzyme activity in skeletal muscle. *J Biol Chem* **242**, 2278–2282.

Horowitz JF, Coppack SW, Paramore D, Cryer PE, Zhao G & Klein S (1999). Effect of short-term fasting on lipid kinetics in lean and obese women. *Am J Physiol Endocrinol Metab* **276**, E278–284.

Houmard JA, Tanner CJ, Yu C, Cunningham PG, Pories WJ, MacDonald KG & Shulman GI (2002). Effect of weight loss on insulin sensitivity and intramuscular long-chain fatty acyl-CoAs in morbidly obese subjects. *Diabetes* **51**, 2959–2963.

Jagoe R & Goldberg A (2001). What do we really know about the ubiquitin-proteasome pathway in muscle atrophy? *Curr Opin Clin Nutr Metab Care* **4**, 183–190.

Lee SD, Tzang BS, Kuo WW, Lin YM, Yang AL, Chen SH, Tsai FJ, Wu FL, Lu MC & Huang CY (2007). Cardiac fas receptor-dependent apoptotic pathway in obese Zucker rats. *Obesity (Silver Spring)* **15**, 2407–2415.

Lee SW, Dai G, Hu Z, Wang X, Du J & Mitch WE (2004). Regulation of muscle protein degradation: coordinated control of apoptotic and ubiquitin-proteasome systems by phosphatidylinositol 3 kinase. *J Am Soc Nephrol* **15**, 1537–1545.

Lillioja S, Young A, Culter C, Ivy L, Abbott W, Zawadzki J, Yki-Jarvinen H, Chnstin L, Secomb T & Bogardus C (1987). Skeletal muscle capillary density and fiber type are possible determinants of in vivo insulin resistance in man. *J Clin Invest* **80**, 415–424.

Lin J, Wu H, Tarr PT, Zhang C-Y, Wu Z, Boss O, Michael LF, Puigserver P, Isotani E, Olson EN, Lowell BB, Bassel-Duby R & Spiegelman BM (2002). Transcriptional co-activator PGC-1a drives the formation of slow-twitch muscle fibres. *Nature* **418**, 797–801.

Maiuri MC, Zalckvar E, Kimchi A & Kroemer G (2007). Self-eating and self-killing: crosstalk between autophagy and apoptosis. *Nat Rev Mol Cell Biol* **8**, 741–752.

Mammucari C, Milan G, Romanello V, Masiero E, Rudolf R, Del Piccolo P, Burden SJ, Di Lisi R, Sandri C, Zhao J, Goldberg AL, Schiaffino S & Sandri M (2007). FoxO3 controls autophagy in skeletal muscle in vivo. *Cell Metabolism* **6**, 458–471.

Minnaard R, Drost M, Wagenmakers A, van Kranenburg G, Kuipers H & Hesselink MKC (2005). Skeletal muscle wasting and contractile performance in septic rats. *Muscle Nerve* **31**, 339–348.

Ozcan U, Hotamisligil GS & Cao Q (2004). Endoplasmic reticulum stress links obesity, insulin action, and type 2 diabetes. *Science* **306**, 457–461.

Pattingre S, Espert L, Biard-Piechaczyk M & Codogno P (2008). Regulation of macroautophagy by mTOR and Beclin 1 complexes. *Biochimie* **90**, 313–323.

Pattingre S, Tassa A, Qu X, Garuti R, Liang XH, Mizushima N, Packer M, Schneider MD & Levine B (2005). Bcl-2 antiapoptotic proteins inhibit beclin 1-dependent autophagy. *Cell* **122**, 927–939.

Preiss J, Loomis CR, Bishop WR, Stein R, Niedel JE & Bell RM (1986). Quantitative measurement of sn-1,2-diacylglycerols present in platelets, hepatocytes, and ras- and sis-transformed normal rat kidney cells. *J Biol Chem* **261**, 8597–8600.

Ryall JG, Gregorevic P, Plant DR, Sillence MN & Lynch GS (2002). β2-Agonist fenoterol has greater effects on contractile function of rat skeletal muscles than clenbuterol. *Am J Physiol Regul Integr Comp Physiol* **283**, R1386–1394.

Ryder JW, Bassel-Duby R, Olson EN & Zierath JR (2003). Skeletal muscle reprogramming by activation of calcineurin improves insulin action on metabolic pathways. *J Biol Chem* **278**, 44298–44304.

Shimabukuro M, Zhou Y-T, Levi M & Unger RH (1998). Fatty acid-induced β cell apoptosis: A link between obesity and diabetes. *Proc Natl Acad Sci U S A* **95**, 2498–2502.

Sinha S, Perdomo G, Brown NF & O'Doherty RM (2004). Fatty acid-induced insulin resistance in L6 myotubes is prevented by inhibition of activation and nuclear localization of nuclear factor κB. *J Biol Chem* **279**, 41294–41301.

Sparangna G & Hickson-bick D (2000). A metabolic role for mitochondria in palmitate-induced cardiac myocyte apoptosis. *Am J Physiol Heart Circ Physiol* **279**, H2124–H2132.

Stitt TN, Drujan D, Clarke BA, Panaro F, Timofeyva Y, Kline WO, Gonzalez M, Yancopoulos GD & Glass DJ (2004). The IGF-1/PI3K/Akt pathway prevents expression of muscle atrophy-induced ubiquitin ligases by inhibiting FOXO transcription factors. *Mol Cell* **14**, 395–403.

Summers SA (2006). Ceramides in insulin resistance and lipotoxicity. *Progr Lipid Res* **45**, 42–72.

Turpin SM, Lancaster GI, Darby I, Febbraio MA & Watt MJ (2006). Apoptosis in skeletal muscle myotubes is induced by ceramides and is positively related to insulin resistance. *Am J Physiol Endocrinol Metab* **291**, E1341–1350.

Unger RH (2003). Minireview: weapons of lean body mass destruction: the role of ectopic lipids in the metabolic syndrome. *Endocrinology* **144**, 5159–5165.

Unger RH, Zhou YT & Orci L (1999). Regulation of fatty acid homeostasis in cells: novel role of leptin. *Proc Natl Acad Sci U S A* **96**, 2327–2332.

Uysal KT, Wiesbrock SM, Marino MW & Hotamisligil GS (1997). Protection from obesity-induced insulin resistance in mice lacking TNF-α function. *Nature* **389**, 610–614.

Van Der Vusse G & Reneman R (1996). Lipid metabolism in muscle. In *Handbook of Physiology:* section 12, *Exercise: Regulation and Integration of Multiple Systems*, ed. Rowell LB & Shepherd JT, pp. 952–994. Oxford University Press, New York.

Warmington S, Tolan R & McBennett S (2000). Functional and histological characteristics of skeletal muscle and the effects of leptin in the genetically obese (ob/ob) mouse. *Int J Obes Relat Metab Disord* **24**, 1040–1050.

Watt MJ, Dzamko N, Thomas WG, Rose-John S, Ernst M, Carling D, Kemp BE, Febbraio MA & Steinberg GR (2006*a*). CNTF reverses obesity-induced insulin resistance by activating skeletal muscle AMPK. *Nat Med* **12**, 541–548.

Watt MJ, Hevener A, Lancaster GI & Febbraio MA (2006*b*). Ciliary neurotrophic factor prevents acute lipid-induced insulin resistance by attenuating ceramide accumulation and phosphorylation of c-Jun N-terminal kinase in peripheral tissues. *Endocrinology* **147**, 2077–2085.

Wei Y, Wang D, Topczewski F & Pagliassotti MJ (2006). Saturated fatty acids induce endoplasmic reticulum stress and apoptosis independently of ceramide in liver cells. *Am J Physiol Endocrinol Metab* **291**, E275–281.

Wellen KE & Hotamisligil GS (2005). Inflammation, stress, and diabetes. *J Clin Invest* **115**, 1111–1119.

Zhao J, Brault JJ, Schild A, Cao P, Sandri M, Schiaffino S, Lecker SH & Goldberg AL (2007). FoxO3 coordinately activates protein degradation by the autophagic/lysosomal and proteasomal pathways in atrophying muscle cells. *Cell Metabolism* **6**, 472–483.

Acknowledgments

We thank Drs Rudolf Zechner and Gunter Haemmerle (University of Graz) for providing the ATGL null mice and Ronnie Minnard for expert technical advice. These studies were supported by research grants from the Australian Research Council (ARC) and the National Health and Medical Research Council (NHMRC) of Australia. S.M.T. is supported by a Dora Lush Scholarship, J.G.R. by a C. J. Martin Postdoctoral Fellowship, M.A.F. by a Principal Research Fellowship and M.J.W. by a R. Douglas Wright Career Development Award from the NHMRC. R.S. is supported by an Australian Post-doctoral Fellowship and B.E.K. a Federation Fellowship from the ARC. A.L.H. is supported by the National Institutes of Health (DK073227).